

# Sketch-Based Face Editing in Videos Using Identity Deformation Transfer

Long Zhao, Fangda Han, Xi Peng, Xun Zhang, Mubbasir Kapadia, Vladimir Pavlovic, and  
Dimitris N. Metaxas, *Fellow, IEEE*

**Abstract**—We address the problem of using hand-drawn sketches to edit the facial identity, such as enlarging the shape or modifying the position of eyes or mouth, in the entire video. This task is formulated as a 3D face model reconstruction and deformation problem. We first introduce a two-stage real-time 3D face model fitting schema to recover the facial identity and expressions from the video. User’s editing intention is recognized from input sketches as a set of facial modifications. Then a novel identity deformation algorithm is proposed to transfer these facial deformations from 2D space to the 3D facial identity directly, while preserving the facial expressions. After an optional stage for further refining the 3D face model, these changes are propagated to the whole video with the modified identity. Both the user study and experimental results demonstrate that our sketching framework can help users effectively edit facial identities in videos, while high consistency and fidelity are ensured at the same time.

**Index Terms**—Sketch-based modeling, video editing, shape deformation, deformation transfer, 3D morphable model



## 1 INTRODUCTION

RECENT years have witnessed tremendous advances in the field of facial performance capture in videos, which serves as a vital foundation for other computer graphics applications [1], [2], [3]. Especially, impressive results have been achieved in state-of-the-art face editing frameworks, and they are widely used in creating funny facial effects for video games, movies and even mobile applications. In order to express user’s editing intention, this kind of frameworks always involves complex inputs (e.g., other images or videos within the same domain [3], [4]) or additional capture devices (e.g., RGB or RGB-D cameras [2], [5], [6]). However, it is quite inconvenient for artists or amateur editors to reach these resources in our daily life. Moreover, current state-of-the-arts always aim to enable users to modify the facial expression of the actor in a video, since this kind of editing intention can be easily detected with fixed facial identities. While changing the identity, i.e., the original appearance of a face without the influence from the pose and facial expression, is quite difficult, since it is a form of modification which is hard to be computed straightforward from reference inputs or some parameters.

We address these two shortcomings by making use of sketch, which offers more efficiency and flexibility to editors as demonstrated in the recent research [7], [8], [9]. Consider the problem of transferring facial characters in a cartoon image to an actor in the video as shown in Fig. 1. In this paper, we propose a novel and robust interactive sketch-based face editing framework for both professional and amateur editors to finish this task very conveniently on a standard PC. *We note that our framework is not a caricature system: the cartoon image we introduced here is not an input which will be processed by our framework; we are simply using it*

*as an inspiration or guideline for users to edit the source video.* In fact, users are free to modify any facial appearance of an actor in the given video with the help of our framework. Compared to previous work, we focus on allowing users to edit the facial identity of the actor in the whole video, but not the expressions.

There are three challenges towards this goal. (1) There is an inherent tradeoff between flexibility of sketch-based specification and robustness. Specifically, unconstrained hand-drawn strokes may produce ambiguous inputs [7], [10]. For example, a stroke drawn between the eyebrow and upper eyelid might indicate editing either of them. And it is quite difficult for the framework to determine the user’s true editing intention by dealing with this stroke alone. (2) Since the face appearance depends on the pose of the actor as well as the identity, the influence of facial expression should be taken into account when applying changes to the identity. (3) Compared with previous sketch-based methods designed for static 2D images or 3D models [7], [8], [10], [11], our framework has to further propagate the modifications from one frame to the whole video. In this process, we need to predict the modified face appearance in each frame while ensuring consistency and fidelity.

In this paper, we introduce a 3D face model fitting and identity deformation transfer formulation. Our core idea is to first transfer modifications from the input sketch to the corresponding 3D face model fitted by the facial identity and expression, which is then used to propagate changes to the whole video. First, we present a two-stage real-time 3D face model fitting algorithm for a sequence input in Sect. 4, which builds on top of prior work [12], [13], while working well on consumer-grade devices. In Sect. 5, a robust sketch mapping and fitting schema is introduced to recognize user’s editing intentions and apply them to the face in 2D space. Specifically, we utilize the order information carried by a series of strokes to mitigate ambiguity. Then an energy function is minimized to deform the face appearance and

• The authors are with the Department of Computer Science, Rutgers University, NJ, USA, 08854.  
E-mail: lz311@cs.rutgers.edu

Manuscript received April 11, 2018.

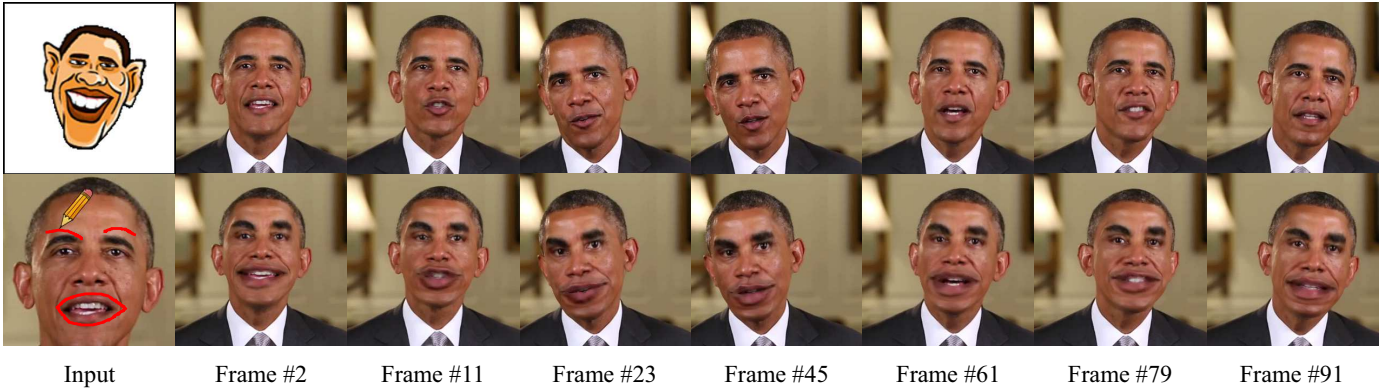


Fig. 1. Given a video, consider the problem of modifying the actor’s facial appearance, e.g. enlarging his mouth, to match facial characters in a reference image (top-left). Our framework enables users to perform such editing operations by hand-drawn sketch. Then these modifications are propagated throughout the whole video. Top: a cartoon image for reference and key frames in a video. Bottom: the input sketches and edited frames. *Note that our framework is not a caricature system. It doesn’t transfer texture styles from cartoon images to videos, since we only focus on sketch-based identity deformation.*

handle stroke noises at the same time. In Sect. 6, we present a novel approach to transfer deformations from 2D space to the 3D facial identity with depth estimation, while get rid of the influence from expression. We also implement a contour-based interface for users to refine the 3D identity optionally in Sect. 7. Finally, Sect. 8 presents the optimization algorithms for rendering the deformed face texture back to the whole video, which removes artifacts generated from the previous steps. User study as well as experiment results shown in Sect. 9 indicate that our sketching framework is simple to use even for amateurs, while high-fidelity results are guaranteed as well.

To the best of our knowledge, we are the first framework which allows users to edit the facial identity of an actor in a video, using sketches. This is made possible with the following key contributions: (1) a sketch-based facial identity editing framework for videos, (2) two-stage real-time 3D face model fitting for a video sequence, (3) robust sketch mapping and fitting, (4) a novel 2D to 3D identity deformation transfer algorithm, (5) and a contour-based interface for 3D model refinement.

## 2 RELATED WORK

**Sketch-Based Shape Editing.** Hand-drawn sketches are widely used in modeling static facial inputs, such as images or 3D shapes [1], [14]. The main challenge of these systems is to handle ambiguous user inputs, i.e., strokes which are difficult to match. Previous work [7], [10], [15] limits the use of only pre-recorded data (curves or points) to mitigate ambiguity. The following two sketch-based facial animation editing systems proposed recently are most related to our work. Nataneli et al. [11] introduced an internal representation of sketch’s semantics, while users have to draw sketch in some predefined regions. Miranda et al. [8] built a sketching interface control system, which only allows users to draw strokes on a predefined set of areas corresponding to different face landmarks to avoid ambiguous conditions. In this paper, we introduce a sketch-based editing framework which differs from previous work in the following two aspects: 1) our method is the first framework that allows users to edit the face by sketch in a video sequence other

than a static image or 3D shape; 2) we utilize the sequence information of strokes to deal with ambiguous user inputs without predefined constraints.

**Parametric Face Model Fitting.** Existing approaches try to solve the problem of parameterizing the 3D face in a given image or video by using either global [7], [13], [16], [17], [18] or local [19], [20], [21], [22], [23] models. In this paper, due to the advantage that our framework does not rely on the face model with high accuracy, we parameterize the global 3D face model based on [13] which is simple but achieves stable results. To fit the 3D face model to a sequence, traditional approaches formulate it by solving a global energy minimization problem [2], [3], [24]. However, since their target equations are highly non-linear, they cannot be solved in real-time. Cao et al. [25] proposed a real-time learning-based approach to regress 3D facial landmarks with fine-scale face wrinkles by a user-specific blendshape model. Other methods [5], [6], [26], [27], [28] are proposed to fit a parametric face model in real-time by using RGB-D data. In this paper, our energy-based formulation to fit the 3D face model is similar to these traditional methods. However, we use a set of linear formulations instead of a global non-linear one and solve it iteratively, which can achieve real-time performance after parallel optimization and can be further applied to streaming inputs.

**Deformation Transfer.** Deformation transfer [29], [30] firstly addressed the problem of transferring local deformations between two different meshes, where the deformation gradient of meshes is directly transferred by solving an optimization problem. Semantic deformation transfer [31] inferred a correspondence between the shape spaces of the two characters from given example mesh pairs by using standard linear algebra. Zhou et al. [32] further utilized these methods to automatically generate a 3D cartoon of a real 3D face. Thies et al. [2] developed a system that transfers expression changes from the source to the target actor based on [29] and achieves real-time performance. Moreover, other flow-based approaches [3], [4] are also proposed to transfer facial expression to different face meshes. However, these traditional methods aim to transfer deformations, especially facial expressions, between 3D meshes. Differing from them,

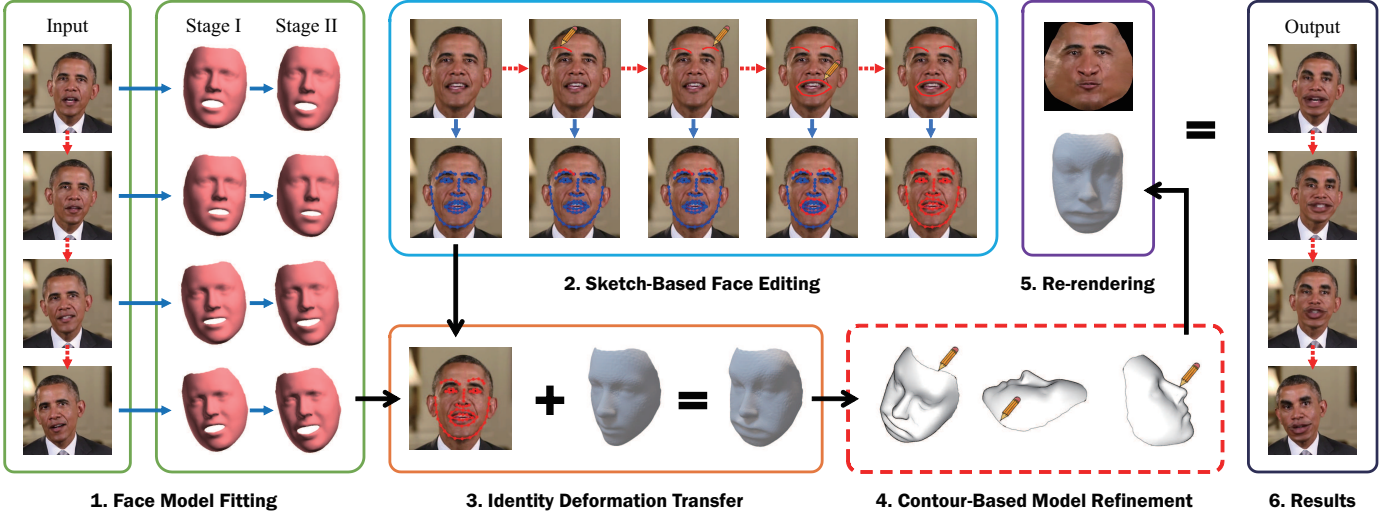


Fig. 2. Workflow of our sketching framework. The detailed algorithm of each part is presented in the corresponding section. Red dashed arrows indicate a sequence of inputs while blue solid arrows stand for model fitting or updating operations, and a dashed box means an optional step.

we propose a transfer pipeline which can be used to directly transfer local identity changes in 2D space to a 3D face model. The main challenge is that there are no direct connections between deformations in different feature spaces. We address this problem by first mapping sketch into a set of modifications corresponding to 3D space, and then transferring it to the target 3D mesh.

### 3 FRAMEWORK OVERVIEW

The input of our framework is a monocular video consisting of continuous frames of a person’s face, together with a certain frame  $t_0$  in this video containing a corresponding hand-drawn sketch. This sketch may be a complete facial sketch or partial strokes representing changes that the user wants to be made to the appearance of the face, e.g., to enlarge the mouth or modify the position of the eyebrows. Our target is to recognize all these changes from the sketch and apply them to the whole video. Inspired by [2], [3], we formulate this task as a parametric face model fitting and deformation transfer problem.

We use the Surrey Face Model based on [12], [13] to fit the face performances in the video. This model contains 63 PCA identity blendshapes  $B_{id} \in \mathbb{R}^{3n \times 63}$ , the mean shape  $\bar{B}_{id} \in \mathbb{R}^{3n}$  and 6 linear expression blendshapes  $B_{exp} \in \mathbb{R}^{3n \times 6}$ . The low-resolution face mesh which has 3448 vertices is employed in this paper. For each frame  $t$ , the face is parameterized as a quadruple  $(\alpha, \beta_t, T_t, M_t)$  by a two-stage fitting algorithm, where  $\alpha \in \mathbb{R}^{63}$  is the global identity coefficient vector,  $\beta_t \in \mathbb{R}^6$  is the expression coefficient vector in this frame,  $T_t$  is the rigid transformation matrix, and  $M_t$  is the isomap [33] extracted from the frame which contains pixel texture information for the face model. Hence, a fully transformed 3D face model  $\mathcal{F}_t$  in the frame  $t$  can be represented as:

$$\mathcal{F}_t(\alpha, \beta_t, T_t) = T_t(\bar{B}_{id} + B_{id} \cdot \alpha + B_{exp} \cdot \beta_t). \quad (1)$$

The core idea proposed in this paper is to represent the facial appearance modifications encoded in the input sketch by a set of local deformations in 2D space, and then transfer them from 2D space to the target 3D identity  $\mathcal{I}$

while removing the influence of expression  $\mathcal{E}_t$  by solving energy minimization problems, where  $\mathcal{I} = \bar{B}_{id} + B_{id} \cdot \alpha$  and  $\mathcal{E}_t = B_{exp} \cdot \beta_t$ . After computing the modified identity shape  $\hat{\mathcal{I}}$ , we can get the updated full 3D face model  $\hat{\mathcal{F}}_t$  for each frame according to Eq. 1. Finally, these modifications are propagated throughout the whole video by rendering  $\hat{\mathcal{F}}_t$  to frame  $t$  with the isomap  $M_t$ . The whole pipeline of our framework is outlined in Fig. 2. In the following, we discuss the individual steps in detail.

### 4 TWO-STAGE REAL-TIME FACE MODEL FITTING

Our 3D face fitting algorithm improves [12], [13] in two ways: (1) our method performs 3D face fitting for videos, while they aim to handle a single image; (2) our method preserves the identity as well as the consistency of the expressions in the whole video. Given a monocular input sequence, we reconstruct all unknown parameters  $(\alpha, \beta_t, T_t)$  jointly within a two-stage iterative optimization schema. In the first stage, we aim to reconstruct  $\alpha$  by first fitting  $\alpha_t$  for each frame  $t$  separately and then merging them into a global identity coefficient vector  $\alpha$ . In the second stage,  $\beta_t$  and  $T_t$  are reconstructed for each frame according to  $\alpha$ .

In the first stage, the values of these unknown parameters are fitted by minimizing the error between the projections of pre-defined landmarks on the 3D face model and their related 2D feature points in the frame. The 2D landmarks are detected and tracked by [34], [35] and then combined into a vector  $y_t = (x_1, y_1, x_2, y_2, \dots, x_K, y_K)^T$  where  $K = 68$ . The projection error term  $E_p$  is defined as the sum of squared errors of the landmark vectors  $x_t$  and  $y_t$

$$E_p = \frac{\|x_t - y_t\|^2}{2\sigma_t^2}, \quad (2)$$

where  $\sigma_t$  is the variance for these landmark points, and  $x_t$  is the combined vector of all 2D projection of the 3D landmarks using the estimated transformation matrix. Specifically, the coordinate  $x_t^{(i)}$  of the  $i$ -th point in  $x_t$  is defined as  $x_t^{(i)} = T_t(\bar{B}_{id}^{(i)} + B_{id}^{(i)} \cdot \alpha_t + B_{exp}^{(i)} \cdot \beta_t)$ , where  $\bar{B}_{id}^{(i)}$ ,  $B_{id}^{(i)}$  and  $B_{exp}^{(i)}$  represent related blendshape components which only

contain the rows corresponding to the  $i$ -th landmark point. We define the total energy function in the first stage as:

$$E_f^1 = E_p + w_\alpha E_n(\alpha_t) + w_\beta E_n(\beta_t), \quad (3)$$

where  $E_n(\cdot) = \frac{1}{2} \|\cdot\|^2$  is a regularization term to force the new shape to be close to the distribution of the prior blendshapes to avoid unrealistic results;  $w_\alpha$  and  $w_\beta$  are parameters leveraging the tradeoff between different terms, and they are set to 0.1 experimentally. To minimize Eq. 3, we use coordinate descent: we first solve  $T_t$  using the Gold Standard Algorithm [36] and [37] while fixing the rest, and then come to  $\alpha_t$  and  $\beta_t$ . Finally, another iteration is used to refine the estimates, and the global face coefficient vector  $\alpha$  is computed as the mean of  $\alpha_t$  in each frame.

In the second stage, we fit the final transformation matrix  $T_t$  and the expression coefficient vector  $\beta_t$  for each frame in the same manner as the first stage while  $\alpha_t$  are fixed to  $\alpha$ . The energy function in the second stage is formulated as:

$$E_f^2 = E_p + w_\beta E_n(\beta_t) + w_e E_e, \quad (4)$$

where  $w_e$  is set to 0.2 experimentally, and  $E_e$  is a smooth term for the facial expressions which is designed to ensure that expressions in nearby frames should change smoothly:

$$E_e = \frac{1}{2} \|\beta_t - \beta_{t-1}\|^2. \quad (5)$$

Due to the fact that all the estimations only involve solving a small linear system of equations, the whole fitting algorithm runs in the order of milliseconds. Note that our two-stage fitting algorithm can be extended to deal with streaming inputs, since all the energy functions are formulated based on the current and previous frames.

## 5 SKETCH-BASED FACE EDITING

We present a robust sketch-based face editing framework to enable users to edit all possible face details once they have been marked with the corresponding vertices on the 3D facial identity. In this paper, we allow users to edit 68 face landmarks predefined by [13] for illustration as shown in Fig. 3(b). In order to apply user's editing intention from the input sketch, we need first map each stroke to a suitable part of the face, e.g., the contour of eyes or mouth, and then deform this part according to the stroke.

### 5.1 Sketch Mapping

Our target is to map each stroke to a landmark group in the 2D space (a collection of landmarks which represents a meaningful part of the face, e.g., the left eyebrow or the upper eyelid), and to remove unreasonable strokes from the result at the same time. The main challenge in this task is how to deal with ambiguous user inputs, and Fig. 3(d) shows an example. Previous methods solve this problem by only allowing users to edit the face with predefined curves [7], [10], [15] or draw strokes in pre-ordered regions [8], [11]. Instead, we introduce a robust mapping schema which enables users to draw strokes without certain constraints, while the only assumption we made here is that the stroke should be "clean", i.e., each stroke aims to edit just one target landmark group.

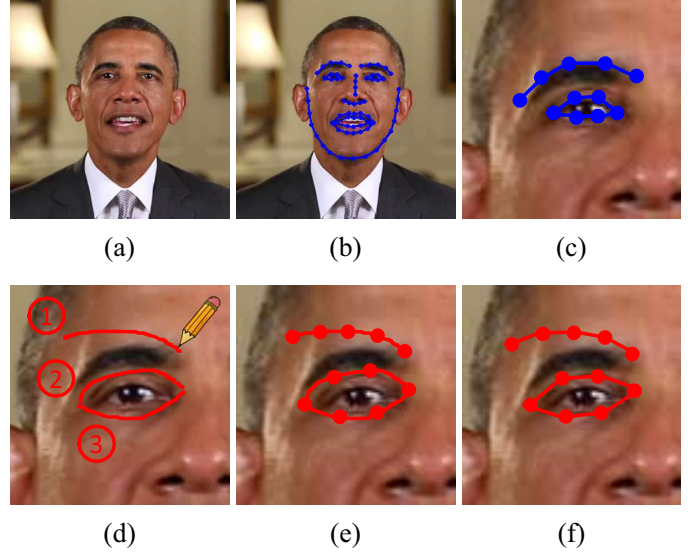


Fig. 3. Illustration of the face landmarks. (a) the original frame; (b) the 68 landmarks predefined by [13]; (c) the original landmarks to be edited; (d) the sketch input (the second stroke is ambiguous since it can be mapped to either the eyebrow or the upper eyelid); (e) key points extracted from the strokes; (f) the final modified landmarks.

We notice users always draw a sketch in a meaningful order encoding their editing intention. Landmark groups having a strong relation with each other, e.g., the upper and bottom eyelids of the same eye, tend to be drawn at the same time. Based on this observation, the input sketch is regarded as an ordered sequence of strokes and Hidden Markov Model (HMM) is employed to formulate this problem. *Note that our HMM-based algorithm leverages the order in which users draw strokes, for efficient matching with landmark groups.* Prior work, e.g., [38] doesn't combine this order information with HMM. It uses HMM to model the shape of this stroke to match mesh templates. Let  $\mathcal{L}$  be a set of landmark groups on the 2D image, and  $S = \{S_1, \dots, S_t\}$  be the stroke sequence of the input sketch. We treat each landmark group  $L$  as the hidden state while a stroke  $S$  is the observation of HMM, and our target is to find the most probable sequence of hidden states (landmark groups) for a given observation sequence (strokes):

$$\arg \max_{L_{1:t}} P(L_{1:t} | S_{1:t}). \quad (6)$$

The initial probabilities  $P(L_0)$  for each hidden state is set to  $\frac{1}{|\mathcal{L}|}$ .  $P(S_t | L_t)$  is the emission probability which measures the probability of each stroke belonging to a certain landmark group. We define  $P(S_t | L_t)$  as:

$$P(S_t | L_t) = \begin{cases} \exp\left(-\frac{d(S_t, L_t)^2}{2\sigma^2}\right), & \text{if } d(S_t, L_t) \leq 3\sigma \\ 0, & \text{otherwise} \end{cases} \quad (7)$$

where  $d(S_t, L_t)$  measures the difference between  $S_t$  and  $L_t$ , which is the average Euclidean distance of their corresponding key points. Note that if  $S_t$  has a high distance with all landmark groups (which means that this stroke is invalid),  $S_t$  will not be matched with any  $L_t$  and excluded from the result.  $P(L_t | L_{t-1})$  is the transition matrix which expresses the probability of moving from one hidden state to another.

Transition probabilities between two landmark groups with a strong relation are assigned a higher value (twice as large as the other values), which makes it easier for corresponding strokes to be mapped at the same time and helps when strokes are ambiguous. Given these parameters, the most probable sequence problem can be solved by the Viterbi Algorithm [39].

## 5.2 Landmark Deformation

For each input stroke  $S$  and its mapped landmark group  $L$ , we need to deform  $L$  into  $\hat{L}$  according to  $S$ , where  $\hat{L}$  is the final modified landmark group. This is achieved by solving an energy minimization function that leverages the position of the input stroke (editing intention of the user) and the original shape of the landmark group. Let  $l_i$  and  $\hat{l}_i$  be the coordinates of the  $i$ -th landmark in  $L$  and  $\hat{L}$  respectively, and  $s_i$  be the corresponding  $i$ -th key point in  $S$ . The target energy function is formulated as:

$$E_k = \underbrace{\sum_{i=1}^n \|\hat{l}_i - s_i\|^2}_{\text{position}} + \underbrace{\sum_{i=1}^{n-1} (1 - \cos(\hat{\gamma}_i - \gamma_i))}_{\text{shape}}, \quad (9)$$

where  $\gamma_i$  is the included angle of  $l_i$  and  $l_{i+1}$ ;  $\hat{\gamma}_i$  is that of  $\hat{l}_i$  and  $\hat{l}_{i+1}$ . To minimize this target function, we use the value of  $\|l_{i+1} - l_i\|$  to approximate  $\|\hat{l}_{i+1} - \hat{l}_i\|$  and solve it with gradient descent.

Intuitively, the position constrain term measures the distance between the modified landmark group and the input stroke, which will move the landmarks of this landmark group to their expected positions. Meanwhile, the shape prior term is employed to maintain the original shape information of this landmark group after the modification, which helps to prevent generating unrealistic results due to noises carried by the input sketch.

## 6 FACIAL IDENTITY DEFORMATION TRANSFER

The final modified facial identity  $\hat{I}$  is calculated from the target identity  $I$  by transferring 2D deformations (a set of modified 2D face landmarks) to  $I$  while taking the influence of expression into consideration. Our strategy is first to estimate the 3D positions of 2D landmarks with reconstructed face model parameters  $(\alpha, \beta_{t_0}, T_{t_0})$ . Then a robust deformation transfer technique is proposed to determine the modified facial identity according to these 3D landmark positions as well as the facial expression. It is achieved by two steps: depth estimation for key points in the 2D space and solving an extended target function of [29]. *The main contribution of our identity deformation transfer algorithm is that we perform the deformation transfer between different feature spaces: from 2D to 3D; while prior work [29], [30], [31] performs the transfer in the same 3D space.*

To estimate the 3D position  $(\hat{x}_i, \hat{y}_i, \hat{z}_i)$  of a certain modified landmark  $\hat{l}_i$  whose 2D coordinate in this frame is  $(\hat{x}_i, \hat{y}_i)$ , we need to reconstruct  $\hat{z}_i$  (the depth of this point towards the screen plane). However, the depth value is unknown since the deformation is made in 2D space. Notice that when the front face is right against the screen plane, i.e., the face plane and screen plane are parallel to each other, points on

the face mesh will have similar depth value (the delta of the maximum and minimum depth value of all the points will reach its minimum), especially for the landmark whose normal vector is perpendicular to the screen plane. Based on this observation, we estimate the depth  $\hat{z}_i$  of the modified landmark  $\hat{l}_i$  with the original depth  $z_i$  of  $l_i$ , which can be computed directly from  $(\alpha, \beta_{t_0}, T_{t_0})$  according to Eq. 1. This estimation can avoid generating unrealistic facial identity effectively. However, as a result, our approach is able to achieve the best performance if the editing is applied on the frame when the actor is facing the camera.

Then we can get the modified facial identity by further transferring deformations (a set of modified 3D landmark coordinates computed above) to the target identity. Our approach is inspired by the correspondence system in [29], but developed in the context of our deformation framework. Let  $\mathcal{V} = \{v_1, \dots, v_n\}$  and  $\hat{\mathcal{V}} = \{\hat{v}_1, \dots, \hat{v}_n\}$  be the  $n$  vertices of the original and modified facial identity. Note that  $\mathcal{V}$  is computed from the facial identity and a pre-defined neutral expression. In this paper, we set all expression parameters to zero to remove the effect of expression as the neutral one for simplicity. We let  $\mathcal{Q}$  be a set of mesh triangles and  $\mathcal{Q}_i = \hat{V}_i V_i^{-1}$  be the affine transformations that define the deformation for the  $i$ -th triangle, where  $\hat{V}_i$  and  $V_i$  are the corresponding vertex matrix [29] calculated from  $\mathcal{V}$  and  $\hat{\mathcal{V}}$  respectively. The vertex positions of the modified identity are computed by minimize the distance between the original and modified 3D landmarks after removing the influence of facial expression. To this end, we define the landmark term as:

$$E_l = \frac{1}{2} \sum_{i=1}^l \|\hat{v}_i - \tilde{l}_i\|^2, \quad (10)$$

where  $l$  is the number of modified 3D landmarks, and  $\tilde{l}_i = \hat{l}_i + B_{exp}^{(i)} \cdot \beta_{t_0}$  is the coordinate of the  $i$ -th modified landmark after merging the influence of facial expression. Then the whole energy function is defined as:

$$E_t(\hat{v}_1, \dots, \hat{v}_n) = w_s E_s + w_i E_i + w_l E_l \quad (11)$$

s.t.  $\hat{v}_k = \mathbf{b}_k, k \in \{1, \dots, m\}$ ,

where  $w_*$  controls the effect of each term, and  $w_i = 0.1$  while the other two are set to 1 experimentally.  $\mathbf{b}_k$  in Eq. 11 is a set of points on the face boundary.  $E_s$  is a smooth term to make the transformations for adjacent triangles be similar with each other [29]:

$$E_s(\hat{v}_1, \dots, \hat{v}_n) = \frac{1}{2} \sum_{i=1}^{|\mathcal{Q}|} \sum_{j \in adj(i)} \|\mathcal{Q}_i - \mathcal{Q}_j\|^2, \quad (12)$$

and  $E_i$  is used to maintain the original triangle shapes which are not affected by the deformation in order to prevent generating a drastic change in the shape of the target identity [29]:

$$E_i(\hat{v}_1, \dots, \hat{v}_n) = \frac{1}{2} \sum_{i=1}^{|\mathcal{Q}|} \|\mathcal{Q}_i - \mathbf{I}\|^2, \quad (13)$$

where  $\mathbf{I}$  is the identity matrix. The whole energy function can be minimized by solving a system of linear equations. During this procedure, the boundary points of the deformed mesh will match exactly since they are specified as constraints to keep the original face contour, the local

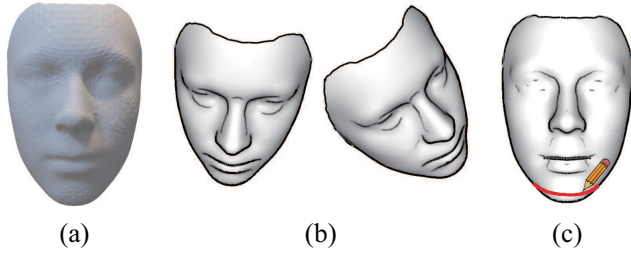


Fig. 4. We provide a contour-based mode for model refinement. Given a 3D face mesh (a), a hybrid line rendering method is utilized to render the contours from different view points (b). Users are allowed to edit these contours with sketches as shown in (c).

deformations are transferred by the landmark term, and the rest of the mesh will be carried along by the smoothness and identity terms.

## 7 CONTOUR-BASED FACE MODEL REFINEMENT

Since the quality of a 3D face model computed from the identity deformation transfer highly influences our final result, we implement an interface for artists to directly edit the deformed 3D face model for refinement. To ensure fluency and simplicity of user interaction during this process, we present a contour-based editing schema. Note that this optional refinement step can be skipped if a favorable result has already been achieved during previous steps or users have no experience in 3D model editing.

At the beginning of this refinement stage, selected feature contours on the deformed 3D face model are projected onto the 2D canvas to produce an initial sketch-like contour map. Then the user can drag or rotate it to observe the model from different views. If some of the projected lines are not satisfactory, the user can redraw them with new sketches. In this refinement phase, these redrawn lines are matched more closely with user inputs by adding them as new constraints for the 3D face model. Compared with traditional interactive 3D mesh editing softwares such as MAYA or 3DS-MAX, which always take a long time for a skilled artist to create a decent 3D face model, our contour-based approach is much simpler and faster. Moreover, this contour-based refinement stage also ensures a smooth user experience during the whole editing process for not involving different softwares or interactive modes other than hand-drawn sketches.

**Contour Rendering.** Recent studies [40], [41] present a hybrid line rendering method to generate 2D contour maps for 3D shapes and obtain good performance. In this paper, we adopt this approach which combines predefined exterior silhouettes, occluding contours, suggestive contours [42] and shape boundaries to generate the final contour map from a given view point for further editing. Examples are shown in Fig. 4. Note that the preprocess steps in [43] are also applied to reduce the noise in the initial map.

**3D Model Refinement.** Users are allowed to rotate the input 3D model to edit its 2D contour map from different view points. Once an unsatisfactory line in the map is found, users can modify it by marking a certain region around to erase it first, and draw a new relevant sketch. After sampling the key points from them, the edited line is then calculated



Fig. 5. We use the refined isomap (the second row) to remove artifacts. From left to right: the original frame and the sketch input, texture isomap, the modified output, detailed view of the output.

by the same algorithm as described in Sect. 5.2. We treat the key points in the edited line as new landmark constraints, and the identity deformation transfer in Sect. 6 is employed to update the face model. Users are able to repeat these steps until a favourable 3D facial identity  $\hat{I}$  is achieved. Note that since more constraints are added, we increase the weights of  $w_s$  and  $w_i$  in Eq. 11 at this stage so as to prevent drastic deformations in the final 3D shape  $\hat{I}$ .

## 8 TEXTURE RE-RENDERING AND SMOOTHING

Propagating deformations to the whole video is achieved by computing modified  $\hat{\mathcal{F}}_t$  with  $\hat{I}$  for each frame  $t$  according to Eq. 1, and then re-rendering the extracted face texture isomap  $M_t$  back to the frame with  $\hat{\mathcal{F}}_t$ . For a high-fidelity result, the background should be warped as well, so that both sides of the face boundary deform coherently. Moreover, we also apply the median filter on the boundary to further blur the difference between the face and its surrounding background.

Note that there might be some “holes” (invisible pixels) on the isomap  $M_t$  due to the occlusion. However, if modifications are applied on the boundary of the 3D facial identity, these “holes” will lead to artifacts after smoothing since they might be visible as a result of the deformation. We notice that these missing pixels may be seen from other frames (since the actor always have different poses in different frames), which can be used to fill “holes” in one certain frame. Therefore, we utilize a refined isomap  $\hat{M}_t$  to synthesize the modified face in each frame. To obtain the refined isomap  $\hat{M}_t$ , we first compute a mean isomap  $\bar{M}$  from all frames in the given video. And then for the isomap  $M_t$  of each frame  $t$ , we use this mean isomap to fill the “holes” in it. We obtain the final refined isomap  $\hat{M}_t$  for each frame after applying a Gaussian filter on it to smooth the boundaries. Finally, the artifacts on the boundary can be removed by re-rendering the face with  $\hat{M}_t$  as shown in Fig. 5.

To handle missing background due to the facial deformation, one simple strategy is building a background model (background as in non-face and non-body) over successive frames and then replacing missing background pixels with newly revealed ones. However, this approach depends on

TABLE 1  
Average Runtime of Our Framework

Video Quality	360P	480P	720P	1080P
Model Fitting	11.9ms	12.1ms	13.6ms	14.3ms
Sketch Matching	1.4ms	1.4ms	1.8ms	2.1ms
Deform Transfer	3.1ms	3.1ms	3.4ms	3.5ms
Texture Rendering	16.6ms	20.5ms	82.6ms	98.6ms
Background Optimization	18.8ms	21.6ms	28.1ms	34.2ms
FPS	<b>29.3Hz</b>	<b>26.9Hz</b>	9.7Hz	8.4Hz
FPS w/ BG Opt.	19.2Hz	16.8Hz	7.6Hz	6.2Hz

**Note:** The average runtime for one frame of each step in our method is computed with respect to different video resolutions. The program runs on the CPU after parallel optimization.

an accurate background segmentation algorithm. In this paper, we solve it in a more robust warping-based manner. Firstly, we employ SIFT [44] to detect the static key points from the starting frame; optical flow is calculated throughout the whole video in order to track the dynamic key points of the background. Then we construct a set of control points for each frame by combining the static and dynamic points. Finally, we use Moving Least Square [45] algorithm to warp the background pixels based on detected control points. This optimization strategy can effectively avoid shaking for static objects in the background, while maintain the consistency of the face boundary concurrently.

## 9 RESULTS

We evaluate the performance of our approach on different Youtube videos at a resolution of  $1280 \times 720$ . The videos show different actors with different scenes captured from varying camera angles; we choose one frame for each video and provide a corresponding sketch of the actor’s face as the input. In our experiments, users are allowed to edit 68 face landmarks marked by [13] by sketch for demonstration. Example results created by amateurs using our sketching interface are shown in Fig. 1 and Fig. 6.

### 9.1 Runtime Performance

We evaluate the runtime performance of our methods by computing the average runtime of each step with respect to different video resolutions. In face model fitting, we run two iterations for both two stages. Within the step of texture re-rendering, an isomap with  $256 \times 256$  resolution is computed for 360P and 480P videos;  $512 \times 512$  resolution is configured for HD videos. Our approach runs on a desktop computer with an Intel 4.00GHz Core i7-6700K CPU. Table 1 shows the result. The texture re-rendering and background optimization is the slowest components, while others run in a matter of milliseconds. Note that our framework can achieve real-time performance ( $\geq 25$  FPS) for standard resolution videos without background optimization, which is compatible with streaming inputs. Moreover, our method does not rely on a power GPU and can be extended to light-weight devices.

### 9.2 User Study

In this section, the user study is conducted to evaluate the user experience as well as the video results achieved by our

framework. We invited 20 people, 10 men and 10 women. All participants are graduate students aged from 23 to 25, and 3 of them major in arts while the others come from statistics and computer science departments. In addition, 4 of them have background in arts and 3D animation modeling (with 3-year experiences in MAYA and 3DS-MAX as well), while the others are amateur users that have limited or no knowledge about drawing and 3D editing. Before the following sessions, a 10-minute tutorial as well as 20 minutes for practice were given to guarantee that every participant knows how to use our interface. Another 40 minutes are employed to introduce MAYA to amateur users. In our evaluation, we use cartoon images as reference to compare our results with users’ true editing intention in an effective way. Users are asked to edit the face to match a cartoon image using our system. However, they are free to make additional modifications as they wish. Therefore, the results may contain some unrelated user inputs.

#### 9.2.1 User Experience of Interfaces

The goal of the first session is evaluating the user experience of our sketched-based interface. To guide users’ editing intention, each participant was given a Youtube video together with a 2D cartoon face image as reference, and asked to edit the facial appearance of the actor in this video to match at least one prominent facial character in the cartoon image using our system. Note that the created facial identity was not required to strictly follow the reference image and differences were allowed. All participants should complete 5 tasks in this session with different pairs of videos and reference images as illustrated in Fig. 1 and Fig. 6. We also implemented another deformation-based user interface, where 3D face models were first calculated according to Sect. 4; then MAYA was utilized as the editing tool instead of sketches, and final results were directly generated by the modified models as Sect. 8. In this deformation-based interface, users are only allowed to edit/modify the positions of mesh vertices with MAYA. This constraint is made for fair comparison, since our system deforms the mesh in the same way. All participants were asked to repeat the same tasks with this interface. For amateur users, they could stop anytime if it was too difficult for them to continue while the artists were required to finish all the tasks with it. To verify the effectiveness of our contour-based refinement mode in Sect. 7, the amateur users were recommended to try it after the initial sketching, and the artists should use it for all tasks in this session. At the end of this session, we asked the participants which system is easier to use.

Among all the 16 amateur users, 12 of them finished editing tasks with the deformation-based interface while the others gave up halfway. Instead, all participants completed the same tasks with our sketch-based interface. Moreover, 10 of the amateurs used our contour-based refinement mode; the others chose to skip it for favorable results had already been achieved in the previous steps. In terms of user experience, all participants agree that our system is simpler to use and yields decent results. Those who tried our refinement mode agree that it was very helpful, and the four professional artists agree that it is more efficient than traditional deformation-based software.

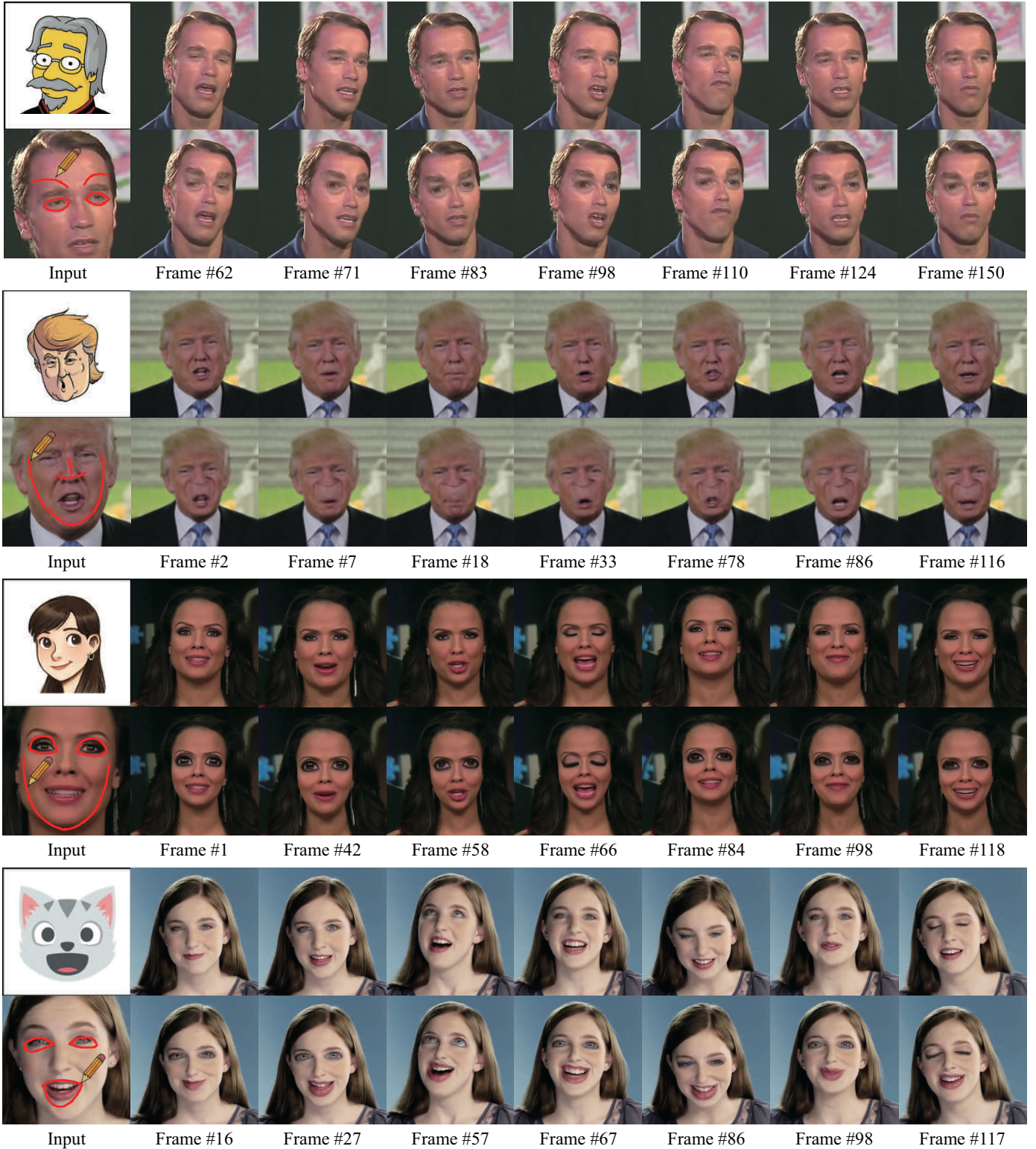


Fig. 6. More examples of our sketching system. In each example, the first column includes the cartoon image for reference (top) and the sketch input (bottom). Starting from the second column, the original (top) and edited frames (bottom) in different videos are shown.

### 9.2.2 Comparison on Mesh Deformation

Fig. 7 shows a gallery of deformed 3D face models, which are corresponding to the actors of the cases as shown in Fig. 1 and Fig. 6, with three different editing interface settings. They were created using our sketch-based interface by amateurs (Ours), by artists with the deformation-based

interface (MAYA\*) and our sketch-based interface with the refinement mode (Ours\*+RF) respectively. Detailed timings are shown in Table 2. In addition, we also report the timing for editing using the deformation-based interface by amateurs (MAYA). As shown in Table 2, an amateur on average only spent 3.6 minutes to complete the task via our system,

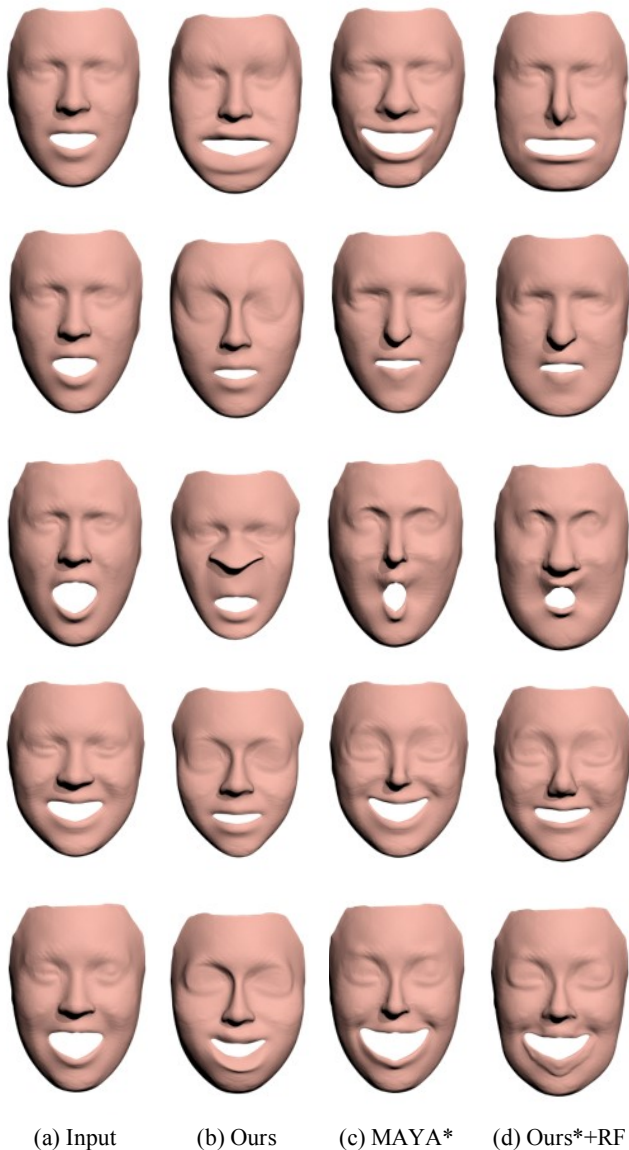


Fig. 7. A gallery of results created using three different editing interface settings. From top to bottom, each row shows the fitted 3D face model and the deformed models corresponding to the cases as shown in Fig. 1 and Fig. 6 respectively. Note that each 3D face model is fitted from the actor in the first frame of the video.

TABLE 2  
Average Timings for Editing with Different Interfaces

Editing Interface	MAYA	Ours	MAYA*	Ours*+RF
Time (min)	12.5 ± 1.8	3.6 ± 0.3	9.5 ± 1.4	4.1 ± 0.8

which is 3 times faster than using the interface based on MAYA. Meanwhile, our sketching interface also doubled the editing efficiency for artists. In Fig. 7, our system is able to achieve results comparable with the ones created using MAYA by artists, while amateurs managed to perform reasonable mesh deformations with our interface.

### 9.2.3 Evaluation on Visual Results

To further evaluate the visual results generated by our sketch-based face editing system, we also designed the second session following the editing session. In this session,

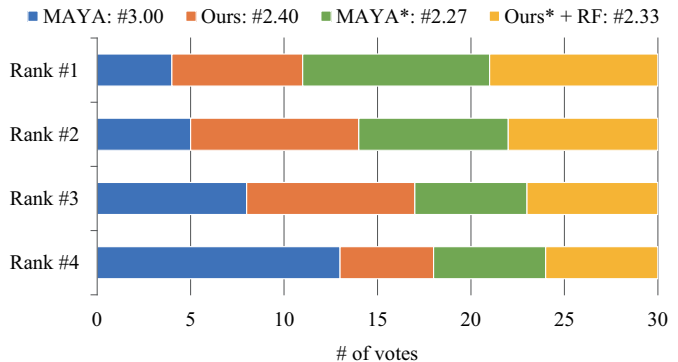


Fig. 8. Voting results from the 1st to 4th rank of videos created with 4 different interface settings. We also report the average ranking of each group following the group name.

results in the previous session were selected into 4 groups: videos edited by amateurs using the deformation-based interface or our sketch-based interface, and ones generated by artists using the deformation-based interface or our sketch-based interface with the refinement mode. For fair comparison, we manually chose the best result in each group for every task in the editing session. After that, all these videos (5 tasks done by 4 groups respectively) together with their corresponding reference cartoon images were presented to additional 30 students who did not participated in the editing session. Given a reference image (displayed in random order), every participant was asked to look at the corresponding videos from the 4 different groups, and then rank them by choosing the one that better matches the cartoon. The final results are shown in Fig. 8.

We can find that videos created by amateurs using our sketching interface obtain higher average rank than ones using deformation-based interface. A T-Test was also conducted to compare rankings obtained with these two different settings. There was a significant difference in the rankings using the deformation-based interface ( $M = 3.00$ ,  $SD = 1.17$ ) and sketch-based interface ( $M = 2.40$ ,  $SD = 1.08$ );  $t(58) = 2.19$ ,  $p = 0.03$ . It demonstrates that our framework does improve the results for amateurs. Notice that different results created by artists and amateurs with our sketching interface have similar average ranks (2.33 and 2.40 respectively). It suggests that, with the help of our sketch-based interface, amateurs manage to create comparable results to a certain extent compared with artists. Another observation is that results have similar ranks when artists use our interface and MAYA, which agrees that artists can produce competitive results with our interface compared with MAYA.

### 9.3 Evaluation of 3D Face Model Fitting

Although face model fitting is not the main focus of our work, we compare our approach with other state-of-the-art methods. The BU-4DFE dataset [46] contains 606 face videos with the resolution of about  $1040 \times 1329$  pixels per frame captured from 101 subjects, which also cover large variances in facial expressions and poses. Videos are captured at a video rate of 25 frames per second, and the average video length is about 100 frames. Each frame comes with a 3D face mesh in the resolution of approximately 35000 vertices

TABLE 3  
Estimation Accuracy and Runtime on BU-4DFE Dataset [46]

Method	3DRMSE	RMSE	Time (s)
TSM [3]	1.93 ± .39	3.81 ± .67	0.579
M3DMM [13]	1.88 ± .55	3.77 ± .62	0.387
Our Method (Stage I)	1.89 ± .40	3.79 ± .35	0.231
Our Method (Stage I and II)	1.86 ± .64	3.72 ± .49	0.325
3DDFA [47]	1.78 ± .44	3.63 ± .56	0.168
RRD [48]	1.72 ± .52	3.53 ± .80	0.118

**Note:** The top four methods are CPU-based without parallel optimization, and the bottom two are learning-based approaches using GPUs. 3DRMSE and RMSE are measured in real-world mm, and lower values are better. Note that 3D models with the highest resolution are utilized.

as the ground truth. We randomly selected 50 videos with different subjects from this dataset for evaluation.

We compare our method with four state-of-the-arts: two CPU-based algorithms: TSM [3], M3DMM [13], and two deep learning methods: 3DDFA [47], RRD [48]. Ours and M3DMM make use of the Surrey Face Model [13] and others employ the Basel Face Model [49] for 3D face model fitting. To be fair, the meshes with the highest resolution offered by both models are used for evaluation, and all CPU-based methods are run without parallel optimization. We follow the experiment settings of [48] to compute the estimation errors of each method by two standard measures: 3D Root Mean Square Error (3DRMSE) and Root Mean Square Error (RMSE). Detailed results are shown in Table 3. All methods are run on a desktop computer with Intel 4.00GHz Core i7-6700K CPU and GTX 1060.

As shown, our method is able to get comparable results with other state-of-the-arts. Although two learning-based methods obtain better estimation accuracy, they rely on powerful GPUs for calculation. Moreover, our method outperforms other CPU-based methods after the second stage, which demonstrated its effectiveness. *Note that since our method is run via 3D meshes of the highest resolution without CPU parallel optimization in this section, the runtime reported here is slower than the one shown in Table 1.*

#### 9.4 Evaluation of Sketch Matching

To evaluate the performance of sketch matching, we compare our method with a geometry-based algorithm described in [8] and another learning-based approach [11] which both achieve state-of-the-art performance. We use the stroke similarity measurement described in them to match strokes with landmarks respectively as their corresponding approximate implementation. Detailed results are shown in Fig. 9. We can find that all the methods produce competitive results with clear user inputs. However, as shown in the second case of Fig. 9, [8] is sensitive to noises since it fits landmarks to strokes via only geometry features; [11] is able to handle this case due to pre-learned prior knowledge; our method can remove noises by taking the original appearance of the landmark group (the shape prior term in Eq. 9) into consideration. For ambiguous inputs as shown in the third case of Fig. 9, both [8] and [11] map the second stroke to eyebrow incorrectly; we can successfully match it with the upper eyelid since the HMM we employed tends to match

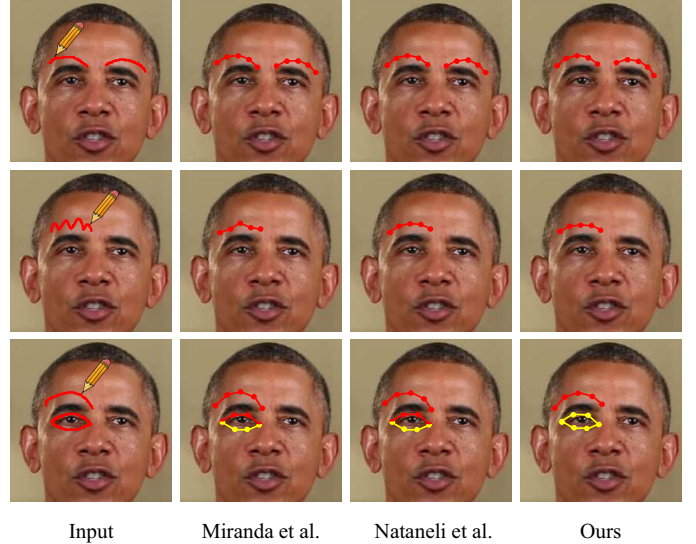


Fig. 9. Comparison of our sketch matching to the approximate implementation of Miranda et al. [8] and Nataneli et al. [11]. From top to bottom: two individual strokes, one stroke with noises, and a group of strokes with ambiguity (different colors represent different matched landmark group pairs). Our method is able to achieve reasonable results for all these cases.

the upper and bottom eyelids at the same time during the optimization.

## 10 CONCLUSION

This paper presents the first sketch-based face editing framework for monocular videos. In an attempt to recognize the user's editing intentions from hand-drawn sketch, a robust sketch matching schema is introduced to convert them to a set of face landmark deformations. Furthermore, a novel facial identity deformation transfer algorithm is employed to propagate these changes throughout the whole video, while consistency and fidelity are maintained. Without background optimization, our framework is able to achieve real-time performance on CPU for streaming inputs with standard definition. Overall, we believe our framework will contribute to many new and exciting applications in the field of face editing on light-weight devices, e.g., a tablet PC and mobile phone.

**Limitations.** Simple interface and good runtime performance are two important principles guide the design of our algorithm. Although using more complex PCA model (e.g., FaceWarehouse [50]) and post-processing steps (e.g., removing blurs and refining backgrounds) improve the final visual results, it will need more runtime. We find that the current setting in this paper can achieve favorable results for standard resolution videos at interactive rates.

There are some notable limitations to our work. One limitation of our sketch-mapping algorithm is that amateur users may not produce correctly ordered sketches in their first try. We make use of HMM to model the relation of different strokes, and users have to redraw a part of strokes with the incorrect order. However, this is mitigated by the fact that on average, the complexity and number of sketches is small (less than 6 strokes), and our interactive system supports rapid iteration and refinement of strokes.

Another limitation is that we only allow users to edit a few landmarks on a face. This is due to the limitation of the morphable models we employed to construct the 3D face: local geometric details such as wrinkles cannot be represented. Moreover, since our method relies on a fixed z-value for more accurate depth estimation, users have to draw sketches on a front face to achieve the best performance.

**Future Work.** In the future, we will consider implementing a stereo editing interface to enhance the user experience and enable users to edit faces from different view points as well. To alleviate the problem of limited editing ability, we propose to utilize Generative Adversarial Network (GAN) [51] to make pixel-to-pixel prediction directly from sketches instead of using morphable models. Moreover, allowing users to edit more facial details from sketches is another future direction. We expect other interesting applications for the framework we have shown here. One can imagine coupling this work with an artist to create a cartoon talking avatar starting from a video.

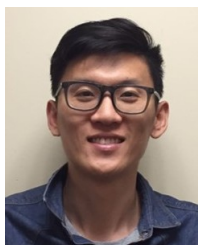
## REFERENCES

- [1] X. Han, C. Gao, and Y. Yu, "DeepSketch2Face: A Deep Learning Based Sketching System for 3D Face and Caricature Modeling," *ACM Transactions on Graphics (TOG)*, vol. 36, no. 4, pp. 126:1–126:12, 2017.
- [2] J. Thies, M. Zollhöfer, M. Stamminger, C. Theobalt, and M. Nießner, "Face2Face: Real-time Face Capture and Reenactment of RGB Videos," in *IEEE Conference on Computer Vision and Pattern Recognition (CVPR)*, 2016.
- [3] F. Yang, L. Bourdev, E. Shechtman, J. Wang, and D. Metaxas, "Facial Expression Editing in Video Using a Temporally-Smooth Factorization," in *IEEE Conference on Computer Vision and Pattern Recognition (CVPR)*, 2012.
- [4] F. Yang, J. Wang, E. Shechtman, L. Bourdev, and D. Metaxas, "Expression Flow for 3D-aware Face Component Transfer," *ACM Transactions on Graphics (TOG)*, vol. 30, no. 4, pp. 60:1–60:10, 2011.
- [5] Y.-L. Chen, H.-T. Wu, F. Shi, X. Tong, and J. Chai, "Accurate and Robust 3D Facial Capture Using a Single RGBD Camera," in *International Conference on Computer Vision (ICCV)*, 2013, pp. 3615–3622.
- [6] P.-L. Hsieh, C. Ma, J. Yu, and H. Li, "Unconstrained realtime facial performance capture," in *IEEE Conference on Computer Vision and Pattern Recognition (CVPR)*, 2015, pp. 1675–1683.
- [7] M. Lau, J. Chai, Y.-Q. Xu, and H.-Y. Shum, "Face Poser: Interactive Modeling of 3D Facial Expressions Using Facial Priors," *ACM Transactions on Graphics (TOG)*, vol. 29, no. 1, pp. 3:1–3:17, 2009.
- [8] J. C. Miranda, X. Alvarez, J. Orvalho, D. Gutierrez, A. A. Sousa, and V. Orvalho, "Sketch express: A sketching interface for facial animation," *Computers & Graphics*, vol. 36, no. 6, pp. 585 – 595, 2012.
- [9] F. Wang, L. Kang, and Y. Li, "Sketch-based 3D shape retrieval using convolutional neural networks," in *IEEE Conference on Computer Vision and Pattern Recognition (CVPR)*, 2015, pp. 1875–1883.
- [10] E. Chang and O. C. Jenkins, "Sketching articulation and pose for facial animation," in *Proceedings of the ACM SIGGRAPH/Eurographics Symposium on Computer Animation*, 2006, pp. 271–280.
- [11] G. Nataneli and P. Faloutsos, "Bringing sketch recognition into your hands," *IEEE Computer Graphics and Applications*, vol. 31, no. 3, pp. 32–41, 2011.
- [12] O. Aldrian and W. A. P. Smith, "Inverse Rendering of Faces with a 3D Morphable Model," *IEEE Transactions on Pattern Analysis and Machine Intelligence*, vol. 35, no. 5, pp. 1080–1093, 2013.
- [13] P. Huber, G. Hu, R. Tena, P. Mortazavian, W. P. Koppen, W. Christmas, M. Rätzsch, and J. Kittler, "A Multiresolution 3D Morphable Face Model and Fitting Framework," in *International Conference on Computer Vision Theory and Applications (VISAPP)*, 2016.
- [14] L. Olsen, F. F. Samavati, M. C. Sousa, and J. A. Jorge, "Sketch-based modeling: A survey," *Computers & Graphics*, vol. 33, no. 1, pp. 85–103, 2009.
- [15] T. Suontphunt, Z. Mo, U. Neumann, and Z. Deng, "Interactive 3D Facial Expression Posing Through 2D Portrait Manipulation," in *Proceedings of Graphics Interface*, 2008, pp. 177–184.
- [16] V. Blanz and T. Vetter, "A Morphable Model for the Synthesis of 3D Faces," in *SIGGRAPH*, 1999, pp. 187–194.
- [17] G. Hu, F. Yan, C.-H. Chan, W. Deng, W. Christmas, J. Kittler, and N. M. Robertson, "Face Recognition Using a Unified 3D Morphable Model," in *European Conference on Computer Vision (ECCV)*, 2016, pp. 73–89.
- [18] T. F. Cootes, G. J. Edwards, and C. J. Taylor, "Active appearance models," *IEEE Transactions on Pattern Analysis and Machine Intelligence*, vol. 23, no. 6, pp. 681–685, 2001.
- [19] P. Joshi, W. C. Tien, M. Desbrun, and F. Pighin, "Learning controls for blend shape based realistic facial animation," in *Proceedings of the ACM SIGGRAPH/Eurographics Symposium on Computer Animation*, 2003, pp. 187–192.
- [20] K.-G. Na and M.-R. Jung, "Local shape blending using coherent weighted regions," *The Visual Computer*, vol. 27, no. 6, p. 575, 2011.
- [21] T. Neumann, K. Varanasi, S. Wenger, M. Wacker, M. Magnor, and C. Theobalt, "Sparse localized deformation components," *ACM Transactions on Graphics (TOG)*, vol. 32, no. 6, pp. 179:1–179:10, 2013.
- [22] C. Wu, D. Bradley, M. Gross, and T. Beeler, "An Anatomically-constrained Local Deformation Model for Monocular Face Capture," *ACM Transactions on Graphics (TOG)*, vol. 35, no. 4, pp. 115:1–115:12, 2016.
- [23] A. Brunton, T. Bolkart, and S. Wuhler, "Multilinear Wavelets: A Statistical Shape Space for Human Faces," in *European Conference on Computer Vision (ECCV)*, 2014, pp. 297–312.
- [24] F. Shi, H.-T. Wu, X. Tong, and J. Chai, "Automatic Acquisition of High-fidelity Facial Performances Using Monocular Videos," *ACM Transactions on Graphics (TOG)*, vol. 33, no. 6, pp. 222:1–222:13, 2014.
- [25] C. Cao, D. Bradley, K. Zhou, and T. Beeler, "Real-time high-fidelity facial performance capture," *ACM Transactions on Graphics (TOG)*, vol. 34, no. 4, pp. 46:1–46:9, 2015.
- [26] T. Weise, S. Bouaziz, H. Li, and M. Pauly, "Realtime performance-based facial animation," *ACM Transactions on Graphics (TOG)*, vol. 30, no. 4, pp. 77:1–77:10, 2011.
- [27] S. Bouaziz, Y. Wang, and M. Pauly, "Online modeling for realtime facial animation," *ACM Transactions on Graphics (TOG)*, vol. 32, no. 4, pp. 40:1–40:10, 2013.
- [28] H. Li, J. Yu, Y. Ye, and C. Bregler, "Realtime Facial Animation with On-the-fly Correctives," *ACM Transactions on Graphics (TOG)*, vol. 32, no. 4, pp. 42:1–42:10, 2013.
- [29] R. W. Sumner and J. Popović, "Deformation transfer for triangle meshes," *ACM Transactions on Graphics (TOG)*, vol. 23, no. 3, pp. 399–405, 2004.
- [30] M. Botsch, R. Sumner, M. Pauly, and M. Gross, "Deformation transfer for detail-preserving surface editing," in *Vision, Modeling & Visualization*, 2006, pp. 357–364.
- [31] I. Baran, D. Vlastic, E. Grinspun, and J. Popović, "Semantic deformation transfer," *ACM Transactions on Graphics (TOG)*, vol. 28, no. 3, pp. 36:1–36:6, 2009.
- [32] J. Zhou, X. Tong, Z. Liu, and B. Guo, "3D cartoon face generation by local deformation mapping," *The Visual Computer*, vol. 32, no. 6, pp. 717–727, 2016.
- [33] J. B. Tenenbaum, V. d. Silva, and J. C. Langford, "A global geometric framework for nonlinear dimensionality reduction," *Science*, vol. 290, no. 5500, pp. 2319–2323, 2000.
- [34] X. Peng, R. S. Feris, X. Wang, and D. N. Metaxas, "A recurrent encoder-decoder network for sequential face alignment," in *European Conference on Computer Vision (ECCV)*, 2016, pp. 38–56.
- [35] X. Peng, S. Zhang, Y. Yang, and D. N. Metaxas, "Piefa: Personalized incremental and ensemble face alignment," in *International Conference on Computer Vision (ICCV)*, 2015, pp. 3880–3888.
- [36] R. Hartley and A. Zisserman, *Multiple View Geometry in Computer Vision*, 2nd ed. Cambridge University Press, 2003.
- [37] X. Peng, J. Huang, Q. Hu, S. Zhang, A. Elgammal, and D. Metaxas, "From circle to 3-sphere: Head pose estimation by instance parameterization," *Computer Vision and Image Understanding*, vol. 136, pp. 92–102, 2015.
- [38] V. Kraevoy, A. Sheffer, and M. van de Panne, "Modeling from contour drawings," in *Proceedings of the 6th Eurographics Symposium on Sketch-Based Interfaces and Modeling*, 2009, pp. 37–44.

- [39] A. Viterbi, "Error bounds for convolutional codes and an asymptotically optimum decoding algorithm," *IEEE transactions on Information Theory*, vol. 13, no. 2, pp. 260–269, 1967.
- [40] F. Wang, L. Lin, and M. Tang, "A new sketch-based 3D model retrieval approach by using global and local features," *Graphical Models*, vol. 76, no. 3, pp. 128–139, 2014.
- [41] L. Zhao, S. Liang, J. Jia, and Y. Wei, "Learning best views of 3D shapes from sketch contour," *The Visual Computer*, vol. 31, no. 6, pp. 765–774, 2015.
- [42] D. DeCarlo, A. Finkelstein, S. Rusinkiewicz, and A. Santella, "Suggestive Contours for Conveying Shape," *ACM Transactions on Graphics (TOG)*, vol. 22, no. 3, pp. 848–855, 2003.
- [43] C. L. Zitnick and P. Dollár, "Edge Boxes: Locating Object Proposals from Edges," in *European Conference on Computer Vision (ECCV)*, 2014, pp. 391–405.
- [44] D. G. Lowe, "Distinctive Image Features from Scale-Invariant Keypoints," *International Journal of Computer Vision*, vol. 60, no. 2, pp. 91–110, 2004.
- [45] S. Schaefer, T. McPhail, and J. Warren, "Image deformation using moving least squares," *ACM Transactions on Graphics (TOG)*, vol. 25, no. 3, pp. 533–540, 2006.
- [46] L. Yin, X. Chen, Y. Sun, T. Worm, and M. Reale, "A high-resolution 3D dynamic facial expression database," in *International Conference on Automatic Face and Gesture Recognition (FG)*, 2008.
- [47] X. Zhu, Z. Lei, X. Liu, H. Shi, and S. Li, "Face Alignment Across Large Poses: A 3D Solution," in *IEEE Conference on Computer Vision and Pattern Recognition (CVPR)*, 2016.
- [48] A. T. Tran, T. Hassner, I. Masi, and G. Medioni, "Regressing Robust and Discriminative 3D Morphable Models with a very Deep Neural Network," in *IEEE Conference on Computer Vision and Pattern Recognition (CVPR)*, 2017.
- [49] P. Paysan, R. Knothe, B. Amberg, S. Romdhani, and T. Vetter, "A 3D Face Model for Pose and Illumination Invariant Face Recognition," in *IEEE International Conference on Advanced Video and Signal based Surveillance (AVSS) for Security, Safety and Monitoring in Smart Environments*, 2009.
- [50] C. Cao, Y. Weng, S. Zhou, Y. Tong, and K. Zhou, "FaceWarehouse: A 3D Facial Expression Database for Visual Computing," *IEEE Transactions on Visualization and Computer Graphics (TVCG)*, vol. 20, no. 3, pp. 413–425, 2014.
- [51] I. Goodfellow, J. Pouget-Abadie, M. Mirza, B. Xu, D. Warde-Farley, S. Ozair, A. Courville, and Y. Bengio, "Generative adversarial nets," in *Advances in Neural Information Processing Systems*, 2014, pp. 2672–2680.



**Long Zhao** received his M.S. and B.E. degrees from the School of Software Engineering, both in Tongji University, Shanghai, China. Currently, he is working toward the Ph.D. degree at the Computational Biomedicine Imaging and Modeling Center (CBIM), Rutgers University. His research interests lie primarily in computer vision, computer graphics and machine learning, especially the intersection area between vision and graphics.



**Fangda Han** is a Ph.D. student in the Computer Science Department of Rutgers University. He has been working with Prof. Vladimir Pavlovic since 2016. He received the bachelor's and master's degree in Engineering Physics from Tsinghua University, Beijing, China. His research interests are computer vision and machine learning.



**Xi Peng** is a research associate at Rutgers University. He received the B.S. degree in Automation Science from Beihang University, China in 2008, the M.S. degree in Computer Science from Chinese Academy of Sciences, China in 2011, and the Ph.D. degree in Computer Science from Rutgers University, U.S. in 2017. He served as a research engineer in Baidu during 2011-2012. His research interests mainly focus on computer vision, machine learning, and deep learning. He is a student member of the IEEE.



**Xun Zhang** was a former dedicated indie game developer, amateur photographer and music composer, now pursuing his Ph.D. degree in Computer Science at Rutgers University. His research interests are computer graphics, computer-generated imagery, virtual agents behaviors and embodied conversational agents.



**Mubbasir Kapadia** is an Assistant Professor in the Computer Science Department at Rutgers University. Previously, he was an Associate Research Scientist at Disney Research Zurich. Kapadia's research aims to develop integrated solutions for full-body character animation, planning based control, behavior authoring, and statistical analysis of autonomous virtual human simulations.



modeling and computer vision.

**Vladimir Pavlovic** earned the Ph.D. in electrical engineering at the University of Illinois at Urbana-Champaign in 1999. He was a research scientist at Compaq's Cambridge Research Lab in Cambridge, MA from 1999 until 2001. In 2001 he joined Boston University as a research faculty in the Bioinformatics Program. In 2002 he joined Rutgers as an Assistant Professor in the Department of Computer Science, where he is now a Full Professor. Prof. Pavlovic's research interests include statistical learning, dynamic system



interests include the development of formal methods upon which computer vision, computer graphics, and medical imaging can advance synergistically.

**Dimitris N. Metaxas** received the B.E. degree from the National Technical University of Athens, Athens, Greece, in 1986, the M.S. degree from the University of Maryland, College Park, MD, USA, in 1988, and the Ph.D. degree from the University of Toronto, Toronto, ON, Canada, in 1992. He is currently a Distinguished Professor with the Computer Science Department, Rutgers University, New Brunswick, NJ, USA, where he is directing the Computational Biomedicine Imaging and Modeling Center. His current research